ChemPubSoc Europe
DOI: 10.1002/chem.201303681

Borylated Complexes

Boryl-Functionalized σ-Alkynyl and Vinylidene Rhodium Complexes: Synthesis and Electronic Properties

Holger Braunschweig,*[a] Christopher K. L. Brown,[a] Rian D. Dewhurst,[a] J. Oscar C. Jimenez-Halla,[a, b] Thomas Kramer,[a] Ivo Krummenacher,[a] and Bernd Pfaffinger[a]

Abstract: The synthesis, reactivity, and properties of boryl-functionalized σ-alkynyl and vinylidene rhodium complexes such as *trans*-[RhCl(=C=CHBMes$_2$)(P*i*Pr$_3$)$_2$] and *trans*-[Rh(C≡CBMes$_2$)(IMe)(P*i*Pr$_3$)$_2$] are reported. An equilibrium was found to exist between rhodium vinylidene complexes and the corresponding hydrido σ-alkynyl complexes in solution. The complex *trans*-[Rh(C≡CBMes$_2$)(IMe)(P*i*Pr$_3$)$_2$] (IMe = 1,3-dimethylimidazol-2-ylidene) was found to exhibit solvatochromism and can be quasireversibly oxidized and reduced electrochemically. Density functional calculations were performed to determine the reaction mechanism and to help rationalize the photophysical properties of *trans*-[Rh(C≡CBMes$_2$)(IMe)(P*i*Pr$_3$)$_2$].

Introduction

Borylated molecular and polymeric species have become of great importance due to their broad applications in organic and inorganic synthesis and materials science.[1–10] In particular, the design of π-conjugated organic compounds displaying three-coordinate boron centers is a highly topical area of research, since the functional materials obtained therefrom are promising for use in light-emitting devices, sensors, and electronic circuits.[1–3,5] Metallacumulene complexes have been intensively studied for more than 30 years due to their ability to act as catalysts for olefin metathesis reactions,[11] stereoselective formation of *E* alkenes,[12] and C–N[13] and C–C coupling reactions.[14,15] In the course of this research, metallacumulenes have been functionalized with a broad variety of functional groups to promote specific reactions. In addition, their nonlinear optical properties and physical properties have attracted interest.[16,17]

Nevertheless, the number of boryl-functionalized vinylidene complexes remains limited,[18,19] and no related σ_C-ethynylborane complex has been reported. Herein, we report a simple protocol for the preparation of both Rh^I borylvinylidene and Rh^I σ_C-ethynylborane complexes, as well as the observation of an equilibrium between an Rh^I borylvinylidene complex and its unisolable Rh^{III} σ_C-ethynylborane counterpart. We present an experimental and computational study on the participating reaction mechanisms, as well as the UV/Vis and electrochemical properties of the products. Overall, the results reveal a system in which the oxidation states and bonding modes can be predictably switched by standard synthetic and electrochemical methods. Given the electronic communication between the electrochemically active Rh and B centers in these molecules, the interconversion between the Rh^I vinylidene, Rh^{III} alkynyl, and Rh^I alkynyl species may be useful for the future development of functional boron-containing organometallic complexes with excellent metal–boron communication.

Results and Discussion

Warming a mixture of dimesityl(ethynyl)borane and *cis*-[{Rh(μ-Cl)(P*i*Pr$_3$)$_2$}$_2$] from −40 to −20 °C resulted in a yellow suspension which turned red at about −15 °C (Scheme 1). After

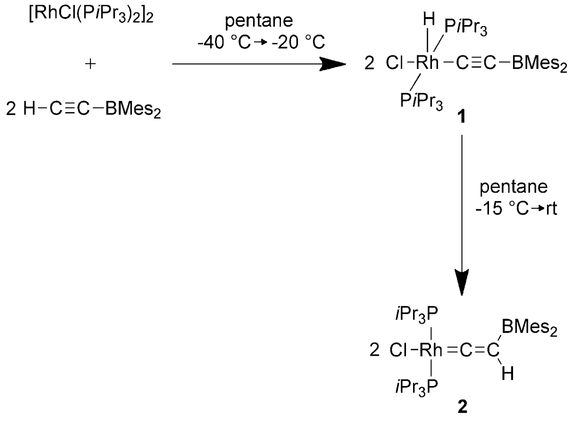

Scheme 1. Formation of **1** and **2**.

---

[a] Prof. Dr. H. Braunschweig, C. K. L. Brown, Dr. R. D. Dewhurst, Dr. J. O. C. Jimenez-Halla, T. Kramer, Dr. I. Krummenacher, Dr. B. Pfaffinger
Institut für Anorganische Chemie
Julius-Maximilians-Universität Würzburg
Am Hubland, 97074 Würzburg (Germany)
E-mail: h.braunschweig@mail.uni-wuerzburg.de

[b] Dr. J. O. C. Jimenez-Halla
Department of Chemistry (DCNE), Universidad de Guanajuato
Noria Alta s/n 36050 Guanajuato (Mexico)

Supporting information for this article is available on the WWW under http://dx.doi.org/10.1002/chem.201303681.

workup at room temperature a red solid (**2**) was isolated which showed a broad $^{11}B\{^1H\}$ NMR signal at 61 ppm and a doublet in the ^{31}P NMR spectrum at 43.9 ppm ($^1J_{PRh}=138.0$ Hz) with a coupling constant typical for rhodium vinylidene complexes ($^1J_{PRh}\approx 140$ Hz).[12] Formation of the vinylidene complex was confirmed by the ^1H NMR spectrum, which showed a singlet at 2.36 ppm for the vinylidene proton. The α-carbon atom of the vinylidene chain was detected in the ^{13}C NMR spectrum at 300.7 ppm as a doublet of triplets ($^1J_{CRh}=60.0$, $^2J_{CP}=12.1$ Hz). The β-carbon atom appeared at 109.4 ppm as a doublet ($^2J_{CRh}=18.0$ Hz).

To assess unequivocally the connectivity of **2**, a single-crystal X-ray diffraction study was carried out (Figure 1). The Rh–C1 (1.775(3) Å) and C1–C2 (1.324(4) Å) distances are comparable to those in the related complex *trans*-$[RhCl(C{=}CHMe)(PiPr_3)_2]$ (Rh–C1 1.775(6), C1–C2 1.32(1) Å) and seem not to be affected by the presence of the boryl group. The C1–C2 (1.324(4) Å) and C2–B (1.544(4) Å) distances of **2** are also longer than those of the parent dimesityl(ethynyl)borane. The boryl group sits at an angle of 48.5(2)° to the C2–C1 axis, and thus conjugation between the boryl group and the vinylidene moiety can be excluded.

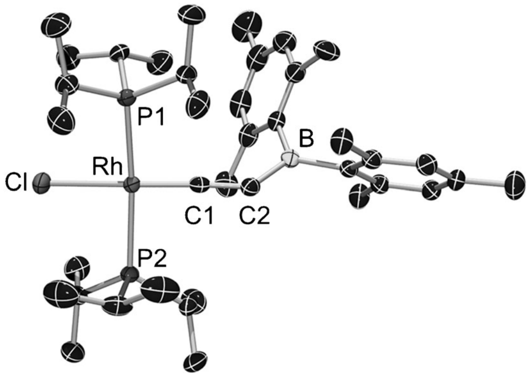

Figure 1. Molecular structure of **2**. Hydrogen atoms have been removed for clarity. Thermal ellipsoids are drawn at 50% probability. Selected bond lengths [Å] and angles [°]: Rh–Cl 2.3837(8), Rh–C1 1.775(3), C1–C2 1.324(4), B–C2 1.544(4); C1-Rh-Cl 176.70(8), C2-C1-Rh 177.5(2), C1-C2-B 131.5(2).

During the synthesis of **2** at low temperatures, we detected intermediate **1** which transforms into **2** on warming to room temperature. In a separate experiment, **1** was isolated and characterized as a yellow solid at low temperature. The yellow temperature-sensitive reaction intermediate **1** was found to be not the respective π-alkyne rhodium(I) complex but the σ-alkynyl hydrido rhodium(III) complex, which shows a doublet of triplets at −27.41 ppm ($^1J_{HRh}=43.7$, $^2J_{HP}=12.0$ Hz) in its ^1H NMR spectrum, and a doublet at 49.5 ppm ($^1J_{PRh}=97$ Hz) in its ^{31}P NMR spectrum. Solid-state IR spectroscopy revealed a C≡C stretching band at 2015 cm^{-1} and thus confirmed the presence of a C≡C bond. The spectroscopic data are comparable with those of *trans*-$[RhHCl(C{\equiv}CFc)(PiPr_3)_2]$ (Fc = ferrocenyl).[20]

An equilibrium between **1** and **2** was observed in benzene at room temperature (Scheme 2). As we were able to monitor the position of the equilibrium by NMR spectroscopy, we attempted to shift the equilibrium to favor the σ-alkynyl hydrido rhodium(III) complex by adding pyridine to generate the octahedral pyridine complex *trans*-$[RhHCl(C{\equiv}CBMes_2)(PiPr_3)_2(py)]$ (**3**; Scheme 3). However, even use of neat pyridine as solvent provided a mixture of **2** and **3**. The octahedral complex **3** is characterized by a broad singlet at −17.8 ppm in the ^1H NMR spectrum, while its ^{31}P NMR spectrum showed a broad doublet around 38 ppm ($^1J_{PRh}=97$ Hz). Both the ^1H and ^{31}P NMR data were consistent with those reported for *trans*-$[RhHCl(C{\equiv}CPh)(PiPr_3)_2(py)]$.[21] Solid-state IR spectroscopy confirmed the existence of a C≡C bond ($\tilde{\nu}=1944$ cm^{-1}).

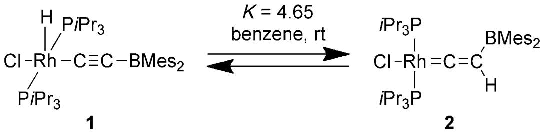

Scheme 2. Equilibrium between **1** and **2**.

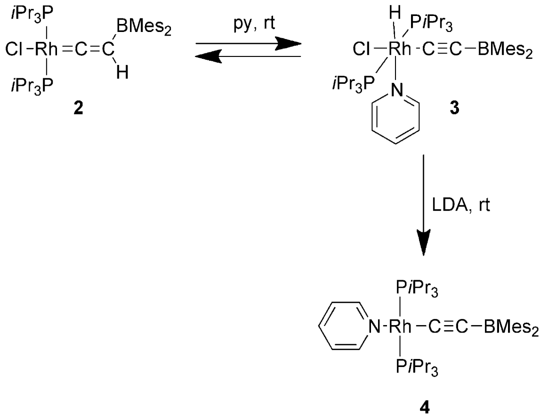

Scheme 3. Reaction of **2** with pyridine to form **3** and subsequent reaction with LDA with formation of **4**.

Elimination of HCl from the rhodium center could be effected by addition of lithium diisopropylamide (LDA) to the reaction mixture, yielding *trans*-$[Rh(C{\equiv}CBMes_2)(PiPr_3)_2(py)]$ (**4**; Scheme 3). This complex was found to decompose slowly when stored in THF solution, and much faster in contact with air, water, or CH_2Cl_2. A singlet at 50.9 ppm was detected in the ^{11}B NMR spectrum of **4** and a doublet at 40.5 ppm in its ^{31}P spectrum ($^1J_{RhP}=149$ Hz). Compound **4** showed a characteristic doublet of triplets at 195.4 ppm ($^1J_{CRh}=45.4$, $^2J_{PC}=22.0$ Hz) for the rhodium-bound alkynyl carbon atom in its ^{13}C NMR spectrum, while the boron-bound alkynyl carbon nucleus was not detected. Solid-state IR spectroscopy revealed a C≡C stretching band at 1934 cm^{-1}.

In contrast to pyridine, the N-heterocyclic carbene 1,3-dimethylimidazol-2-ylidene (IMe) is strong enough to eliminate HCl from **2**, yielding *trans*-$[Rh(C{\equiv}CBMes_2)(IMe)(PiPr_3)_2]$ (**5**; Scheme 4). Compound **5** is stable towards dichloromethane and can be isolated by column chromatography on alumina. In its $^{13}C\{^1H\}$ NMR spectrum, the signal of the rhodium-bound al-

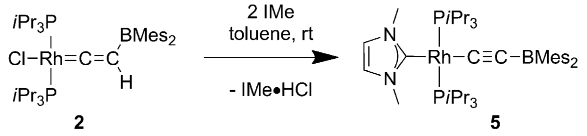

Scheme 4. Reaction of **2** with IMe.

kynyl carbon atom was detected as a doublet of triplets ($\delta = 202.5$ ppm; $^1J_{RhC} = 36.7$, $^2J_{PC} = 22.4$ Hz), and the signal for the NHC carbene carbon nucleus was found at 196.6 ppm ($^1J_{RhC} = 41.30$, $^2J_{PC} = 4.3$ Hz). A doublet at 47.1 ppm ($^1J_{RhP} = 149$ Hz) was detected in its $^{31}P\{^1H\}$ NMR spectrum, and a broad singlet at 52 ppm in its ^{11}B NMR spectrum. IR spectroscopy showed a C≡C stretching band at 1944 cm^{-1}. Overall, the spectroscopic parameters of **4** and **5** are very similar, whereas their stabilities are very different.

To gain more detailed insight into the structural properties of **4** and **5**, both compounds were subjected to single-crystal X-ray diffraction analysis (Figure 2). Both rhodium centers adopt a square-planar geometry. The Rh–C1 distances of the two complexes (**4**: 1.932(2) Å; **5**: 1.983(2) Å) are significantly different, presumably owing to the much stronger σ-donation properties and *trans* influence of the IMe ligand relative to pyridine. The C1–C2 (**4**: 1.242(3) Å; **5**: 1.233(3) Å) distances in both complexes are equivalent within experimental uncertainty. The $BMes_2$ moiety is distorted to a lesser extent from the C1–C2 axis (**4**: 13.1(2)°; **5**: 11.9(2)°) than in **2**. This deviation from expected linearity is most probably caused by the steric bulk of the Mes groups.

As the complexes **2** and **5** turned out to be unexpectedly stable, we subjected them to a more detailed analysis involving both spectroscopic and computational methods. Initially we attempted to explain the observation of hydrido complex **1**, which was isolated as an intermediate in the formation of **2** but also forms an equilibrium with **2** in solution. Thereby, DFT calculations at the M06-2X/'BS2'//M06-2X/'BS1' level of theory were performed (Figure 3; see Supporting Information for further details of the computational methodology). The observation of **1** instead of the respective side-on π-alkyne complex (Reactant) can be explained by the small conversion barrier (**TS1**, 3 kcal mol^{-1}) and by **1** being 6.6 kcal mol^{-1} lower in energy than the side-on complex. The observation of **1** forming an equilibrium with **2** is also attributed to a small energy difference of 2.5 kcal mol^{-1} between the two isomers, in agreement with the observed magnitude of the equilibrium constant and position of the equilibrium. The mechanism of formation of **5** was also clarified. Formation of **5** does not proceed via an octahedral intermediate analogous to **3** followed by elimination of HCl·IMe. Instead, IMe attacks the vinylidene proton, and subsequent elimination of HCl·IMe (energy barrier, **TS2** = 2.6 kcal mol^{-1}) generates a highly unsaturated rhodium(I) center (**Int3**), which immediately reacts with a second equivalent of IMe with formation of **5**. This process (**Int2**→**Product**) is highly energetically favored, as it releases 23.4 kcal mol^{-1} of energy.

Since both **2** and **5** give intensely colored solutions, UV/Vis spectroscopy was performed on solutions of the complexes in hexane (Figure 4). The spectrum of **2** shows absorptions bands at 358 ($\varepsilon = 21\,000$), 292 ($\varepsilon = 19\,000$), and 204 nm (λ_{max}, $\varepsilon = 75\,000$ L mol^{-1} cm^{-1}). The absorption spectrum of **5** is similar to that of **2** with λ_{max} at 205 nm ($\varepsilon = 54\,000$ L mol^{-1} cm^{-1}) and bands at 291 ($\varepsilon = 11\,000$) and 374 nm ($\varepsilon = 14\,000$ L mol^{-1} cm^{-1}). Compound **5** was subjected to a time-dependent DFT (TD-DFT) study in order to assign the absorption bands to the respective transitions (Figure 5). The weak band between 400 and 500 nm is assigned to the HOMO→LUMO transition, and that at 374 nm to the HOMO−1→LUMO transition. With the HOMO being located mostly at the metal center and the LUMO mostly at boron, this can be considered a typical metal-to-ligand charge-transfer transition. The absorption band at 292 nm was found to comprise multiple transitions including HOMO−3→LUMO+1/LUMO and HOMO−2→LUMO+12/LUMO+10.

Compound **5** was also investigated by cyclic voltammetry, which revealed a quasireversible reduction at −3.2 V and a qua-

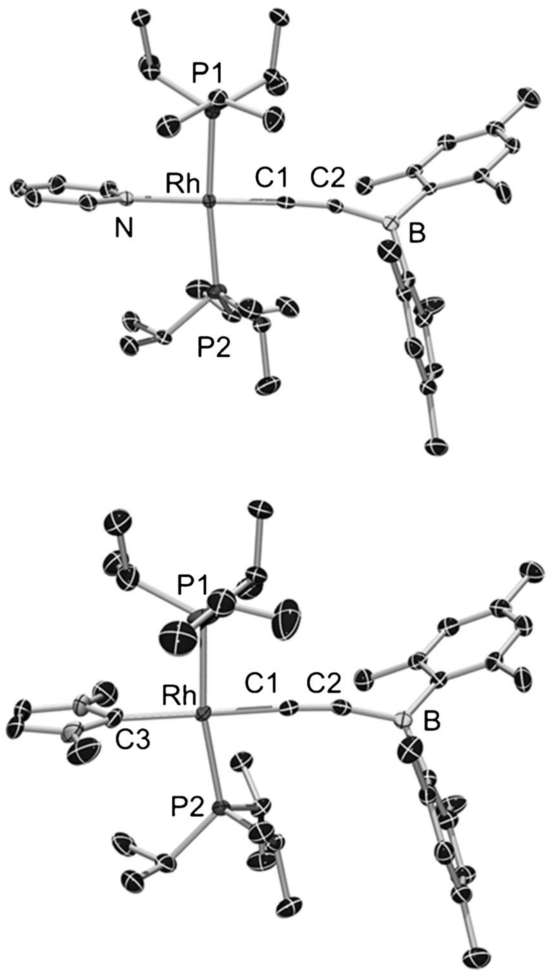

Figure 2. Molecular structures of **4** (top) and **5** (bottom). Hydrogen atoms have been removed for clarity. Thermal ellipsoids are drawn at 50 % probability. Selected bond lengths [Å] and angles [°] for **4**: Rh–N 2.126(2), Rh–C1 1.932(2), C1–C2 1.242(3), B1–C2 1.494(4); C1-Rh1-N 175.10(9), C2-C1-Rh1 174.8(2), C1-C2-B1 166.9(2). Selected bond lengths [Å] and angles [°] for **5**: Rh–C1 1.983(2), Rh–C3 2.058(2), C1–C2 1.233(3), B–C2 1.501(3); C1-Rh-C3 176.23(8), C2-C1-Rh 175.62(17), C1-C2-B 168.1(2).

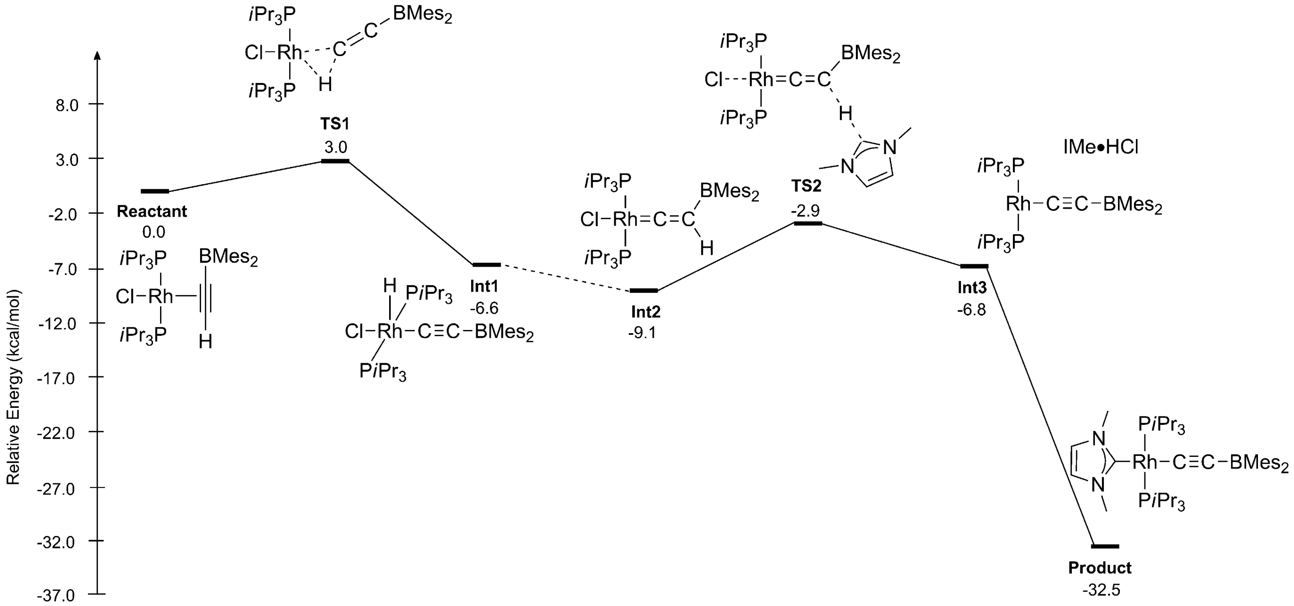

Figure 3. Calculated mechanism of the formation of **5** with Gibbs free energies at 298 K.

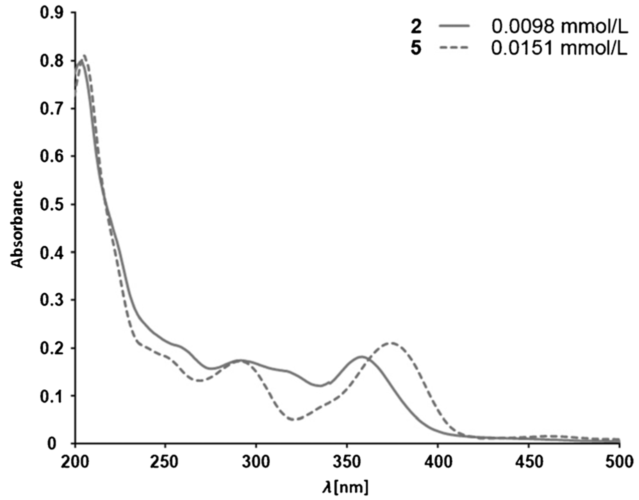

Figure 4. UV/Vis absorption spectra of **2** and **5** in hexane solution.

sireversible oxidation at −0.5 V versus ferrocene/ferrocenium (Fc/Fc$^+$). These two processes are most likely due to the formation of a boron radical and oxidation of the electron-rich Rh^I center, respectively (Figure 6). The reduction potential of **5** is slightly more negative than those of similar neutral boranes such as Mes_3B,[22] which is reduced at $E_{1/2} = -2.9$ V (vs. Fc/Fc$^+$) in THF to radical anion $Mes_3B^{\bullet-}$. This difference can be explained by effective π overlap of the metal alkynyl substituent with the empty boron p_z orbital. The assignment of the redox process at −0.5 V (vs. Fc/Fc$^+$) to a metal-centered oxidation is based on the voltammetric behavior of various other Rh systems, but remains speculative at this point.[23]

To verify the assumed oxidation and reduction processes, Fukui functions were calculated, which showed nucleophilic attack at the metal center and electrophilic attack at the $C{\equiv}CBMes_2$ unit, lending support to our descriptions of the electrochemical processes (Figure 7).

Conclusion

We have reported a convenient synthesis of boryl-functionalized vinylidene complex **2** and were also able to isolate and spectroscopically characterize intermediate hydrido σ-alkynyl complex **1**, which provides insight into the reaction mechanism. Furthermore the reaction of **2** with IMe results in the formation of unusually stable σ-alkynyl complex **5** in an unprecedented manner. Complex **5** shows solvatochromism and can be quasireversibly reduced and oxidized. The experimental work was supported by theoretical calculations, which help to elucidate the mechanism of product formation and the nature of the observed physical phenomena.

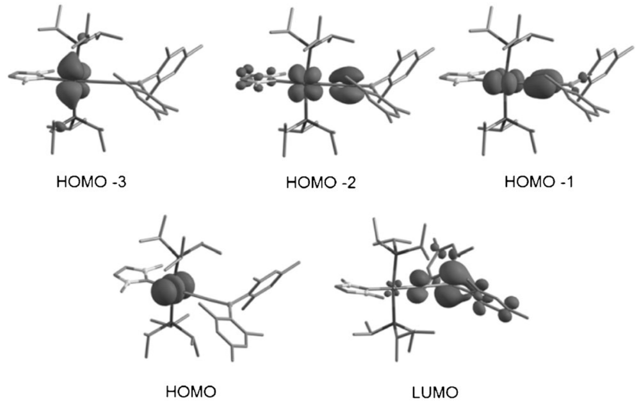

Figure 5. Frontier orbitals of **5**, as derived from DFT calculations.

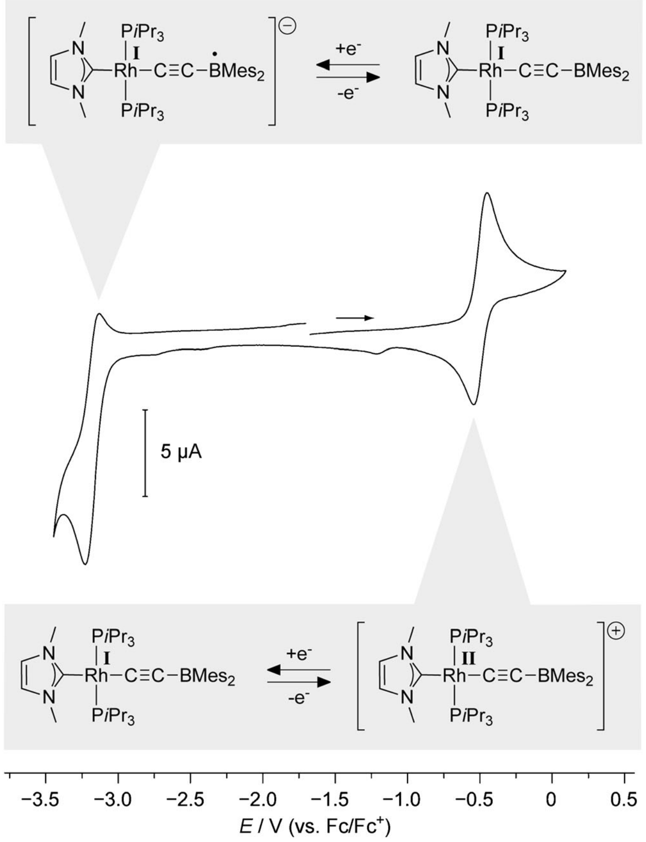

Figure 6. Cyclic voltammogram and presumed electrochemical reduction and oxidation steps for **5**. The CV measurement was performed in THF with 0.1 M $n\mathrm{Bu}_4\mathrm{NPF}_6$ as electrolyte at a scan rate of 300 mV s^{-1}.

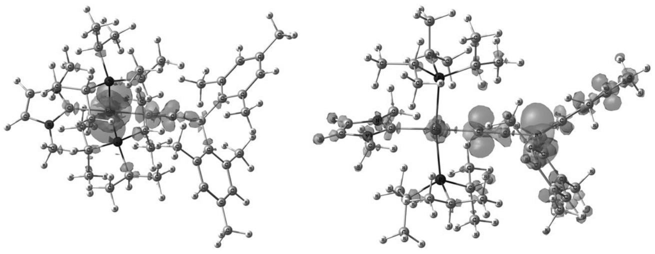

Figure 7. Calculated nucleophilic (f^+, left) and electrophilic (f^-, right) Fukui functions.

Experimental Section

All manipulations were performed under an inert atmosphere of dry argon by using standard Schlenk-line or glovebox techniques. Deuterated solvents were dried over molecular sieves and degassed by three freeze–pump–thaw cycles prior to use. All other solvents were distilled from appropriate drying agents.[24] Solvents were stored under argon over activated molecular sieves. IMe[25] and $[\mathrm{RhCl}(\mathrm{P}i\mathrm{Pr}_3)_2]_2$[26] were prepared according to published procedures. NMR spectra were recorded on a Bruker Avance 500 NMR spectrometer (500.1 MHz for ^{1}H, 160.4 MHz for ^{11}B, 125.76 MHz for ^{13}C{^{1}H}) or Bruker Avance 400 NMR spectrometer (128.38 MHz for ^{11}B). Chemical shifts δ are given in parts per million (ppm) and are referenced against external $\mathrm{Me_4Si}$ (^{1}H, ^{13}C), $\mathrm{H_3PO_4}$ (^{31}P), and $[\mathrm{BF_3{\cdot}Et_2O}]$ (^{11}B). C^q refers to quaternary carbon nuclei. $|N| = {}^1J_{\mathrm{PC}} + {}^3J_{\mathrm{PC}}$ for ^{13}C NMR or $^3J_{\mathrm{PH}} + {}^5J_{\mathrm{PH}}$ for ^{1}H NMR. Infrared data were acquired on a JASCO FT/IR-6200 type A instrument. Melting points were measured with a Mettler Toledo DSC 823. Microanalysis was performed on an Elementar Vario MICRO cube elemental analyzer. Elemental analyses were acquired on an Elementar Vario MICRO cube instrument or a CHNS-932 (Leco). UV/Vis spectra were measured with a JASCO-V660 UV/Vis spectrometer in a quartz glass cell (10 mm). All cyclic voltammetry experiments were conducted in an argon-filled glovebox by using a Gamry Instruments Reference 600 potentiostat. A standard three-electrode cell configuration was employed with a platinum disk working electrode, a platinum wire counter electrode, and a silver wire, separated by a Vycor tip, serving as the reference electrode. Formal redox potentials are reported versus the Fc$^{0/+}$ redox couple, obtained by using ferrocene as internal standard.

Synthesis of 2

A solution of dimesityl(ethynyl)borane in pentane (5.00 mL, 0.828 mmol, $c = 45.0$ mg mL^{-1}) was added dropwise to a solution of $[\{\mathrm{RhCl}(\mathrm{P}i\mathrm{Pr}_3)_2\}_2]$ (380 mg, 0.414 mmol) in pentane (5.00 mL) in a Schlenk tube at room temperature. The orange reaction mixture was stirred for 30 min at room temperature, and all volatile substances were removed under high vacuum. The yellow residue was washed with pentane (2×10.0 mL) at low temperature and subsequently dried under high vacuum at room temperature. Compound **2** was isolated as a red solid (375 mg, 0.511 mmol, 62 %). Single crystals suitable for X-ray analysis were obtained by storing a solution in THF at −70 °C for one week. M.p. 165.8 °C; decomp ≈228.8 °C; ^{1}H NMR (500.1 MHz, $\mathrm{C_6D_6}$, 296 K): $\delta = 6.71$ (s, 4H, m-C$^{\mathrm{Mes}}$H), 2.61–2.56 (m, 6H, PCHCH$_3$), 2.47 (s, 12H, o-C$^{\mathrm{Mes}}$H$_3$), 2.36 (s, 1H, HCBMes$_2$), 2.14 (s, 6H, p-C$^{\mathrm{Mes}}$H$_3$), 1.25 ppm (dvt, 36H, $^2J_{\mathrm{HH}} = 6.7$ Hz, $N = 13.7$ Hz, PCHCH_3); ^{13}C{^{1}H} NMR (125.7 MHz, $\mathrm{C_6D_6}$, 296 K): $\delta = 300.7$ (dt, $^1J_{\mathrm{RhC}} = 60.0$, $^2J_{\mathrm{PC}} = 12.1$ Hz, Rh=C), 139.8 (br s, BC$^{\mathrm{q\text{-}Mes}}$), 137.52 (s, C$^{\mathrm{q\text{-}Mes}}$), 128.86 (s, C$^{\mathrm{Mes}}$H), 109.36 (d, $^2J_{\mathrm{RhC}} = 18.0$ Hz, C=CH), 30.11 (s, p-C$^{\mathrm{Mes}}$H$_3$), 24.90 (vt, $N = 20.3$ Hz, PCHCH$_3$), 24.02 (s, o-C$^{\mathrm{Mes}}$H$_3$), 20.39 ppm (s, PCHCH$_3$); ^{11}B{^{1}H} NMR (160.4 MHz, $\mathrm{C_6D_6}$, 296 K): $\delta = 61$ ppm (s); ^{31}P{^{1}H} NMR (202.4 MHz, $\mathrm{C_6D_6}$, 296 K): $\delta = 43.9$ ppm (d, $^1J_{\mathrm{PRh}} = 138$ Hz); IR (hexane): $\tilde{\nu} = 2956$ (C–H stretch), 1608 (C=C stretch), 1539 cm^{-1} (C=C stretch); UV/Vis (hexane): $\lambda_{\max} = 203.5$ nm ($\varepsilon = 75\,032$ L mol^{-1} cm^{-1}); elemental analysis calcd (%) for $\mathrm{C_{38}H_{65}BClP_2Rh}$: C 62.26, H 8.94; found: C 62.36, H 9.00.

Low-temperature isolation of 1

A solid sample of **1** was prepared analogously to the synthesis of **2**, but the reaction was performed at −40 °C. The temperature of the reaction mixture or solid was not allowed to exceed −20 °C, as the compound is converted to **2** at room temperature. The reaction mixture turned yellow at −30 °C. While warming to −20 °C, all volatile substances were removed under high vacuum. The resulting yellow residue was washed with pentane (5 mL) at −40 °C and subsequently dried under high vacuum at −40 °C. Accordingly, the NMR experiments were performed at low temperatures. ^{1}H NMR (400.1 MHz $\mathrm{CD_2Cl_2}$, 276 K): $\delta = 6.69$ (s, 4H, m-C$^{\mathrm{Mes}}$H), 2.78 (m, 6H, PCHCH$_3$), 2.32–2.22 (m, 12H, o-C$^{\mathrm{Mes}}$H$_3$), 2.21 (s, 6H, p-C$^{\mathrm{Mes}}$H$_3$), 1.22 (dvt, 36H, $^2J_{\mathrm{HH}} = 7.8$ Hz, N = 30.7 Hz, PCHCH_3), −27.41 ppm (dt, 1H, $^1J_{\mathrm{RhH}} = 43.7$, $^2J_{\mathrm{PH}} = 12.0$ Hz, RhH); ^{11}B{^{1}H} NMR (128.38 MHz, $\mathrm{CD_2Cl_2}$, 276 K): $\delta = 59$ ppm (s); ^{31}P{^{1}H} NMR (161.98 MHz, $\mathrm{CD_2Cl_2}$, 276 K): $\delta = 49.5$ ppm (d, $^1J_{\mathrm{RhP}} = 97$ Hz); IR (solid): $\tilde{\nu} = 2015$ cm^{-1} (C≡C stretch).

Synthesis of 3

Compound **2** (47.4 mg, 0.065 mmol) was treated with pyridine (2.00 mL) in a Schlenk tube. The pale yellow solution was stirred for 1 h at room temperature. After slowly evaporating the solvent in a glovebox, the residue was washed with cold pentane (2.00 mL). NMR spectroscopy revealed a mixture of **2** and **3**. ^{1}H NMR (400.1 MHz, C_6D_6, 296 K): $\delta=7.00$–6.70 (m, 5 H, $C^{py}H$), 6.84 (s, 4 H, $C^{Mes}H$), 2.91–2.81 (m, 6 H, $PCHCH_3$), 2.65 (s, 12 H, o-$C^{Mes}H_3$), 2.21 (s, 6 H, p-$C^{Mes}H_3$), 1.16–1.02 (vt, 36 H, $^2J_{HH}=6.5$ Hz, $N=20.3$ Hz, $PCHCH_3$), -17.75 ppm (br s, 1 H, RhH); $^{31}P\{^1H\}$ NMR (161.98 MHz, C_6D_6, 296 K): $\delta=38.5$ ppm (d, $^1J_{RhP}=97.0$ Hz); IR (hexane): $\tilde{\nu}=1944$ (C≡C stretch), 1604 cm^{-1} (C=C stretch).

Synthesis of 4

Compound **2** (47.4 mg, 0.065 mmol) and LDA (6.90 mg, 0.065 mmol) were dissolved in pyridine (3.00 mL) in a Schlenk tube. While stirring the red reaction mixture for 48 h at room temperature, darkening was observed. After removing all volatile substances under high vacuum, the residue was extracted with THF (2.00 mL). After removing all volatile substances under high vacuum, compound **4** was obtained as a red solid, which still contained impurities. Single crystals suitable for X-ray analysis were obtained by slowly evaporating a solution in benzene in a glovebox. M.p. 202.5 °C; decomp >320 °C; ^{1}H NMR (500.1 MHz, C_6D_6, 297 K): $\delta=8.67$–8.65 (m, 2 H, $C^{py}H$), 6.88 (s, 4 H, $C^{Mes}H$), 6.59–6.55 (m, 1 H, p-$C^{py}H$), 6.22–6.19 (m, 2 H, $C^{Py}H$), 2.79 (s, 12 H, o-$C^{Mes}H_3$), 2.25 (s, 6 H, p-$C^{Mes}H_3$), 2.17–2.07 (m, 6 H, $PCHCH_3$), 1.23 ppm (dvt, 36 H, $^2J_{HH}=7.2$ Hz, $N=19.8$ Hz, $PCHCH_3$); $^{13}C\{^1H\}$ NMR (125.7 MHz, C_6D_6, 297 K): $\delta=195.4$ (dt, $^1J_{RhC}=45.4$, $^2J_{PC}=22.0$ Hz), 155.31 (s, $C^{py}H$), 145.95 (s, $C^{q\text{-}Mes}$), 140.17 (s, o-$C^{q\text{-}Mes}$), 135.78 (s, m-$C^{q\text{-}Mes}$), 134.38 (s, p-$C^{py}H$), 128.33 (s, $C^{Mes}H$), 122.96 (s, $C^{py}H$), 25.17 (vt, $N=16.2$ Hz, $PCHCH_3$), 23.64 (s, o-$C^{Mes}H_3$), 21.16 (s, p-$C^{Mes}H_3$), 20.92 ppm (s, $PCHCH_3$); $^{11}B\{^1H\}$ NMR (160.4 MHz, C_6D_6, 297 K): $\delta=50.9$ ppm (s); $^{31}P\{^1H\}$ NMR (202.4 MHz, C_6D_6, 297 K): $\delta=40.5$ ppm (d, $^1J_{RhP}=150$ Hz); IR (solid): $\tilde{\nu}=1934$ cm^{-1} (C≡C stretch).

Synthesis of 5

Compound **2** (90.0 mg, 0.125 mmol) was dissolved in toluene (2.00 mL) in a Schlenk tube. While stirring, a solution of IMe in toluene (2.45 mL, 0.250 mmol, $c=10.0$ mg mL^{-1}) was added by syringe. The red reaction mixture was stirred for 10 min. After removing all volatile substances under high vacuum, the residue was extracted with diethyl ether (2.00 mL) and subjected to column chromatography (Al_2O_3, neutral, activity V, 10 cm) with diethyl ether/pentane (9/1) as eluent. After removing the solvent under vacuum, the residue was washed with cold pentane (3×2.00 mL) and dried under high vacuum. Compound **5** was isolated as a red solid (84.0 mg, 0.110 mmol, 85 %). Single crystals suitable for X-ray analysis were obtained by slowly evaporating a solution in benzene in a glovebox. M.p. 247.6 °C; decomp 271.5 °C; ^{1}H NMR (500.1 MHz, C_6D_6, 296 K): $\delta=6.89$–6.87 (m, 4 H, m-$C^{Mes}H$), 6.05 (s, 2 H, $C^{IMe}H$), 3.50 (s, 6 H, $C^{IMe}H_3$), 2.79 (s, 12 H, o-$C^{Mes}H_3$), 2.36–2.26 (m, 6 H, $PCHCH_3$), 2.25 (s, 6 H, p-$C^{Mes}H_3$), 1.18 ppm (dvt, 36 H, $^2J_{HH}=6.3$ Hz, $N=13.1$ Hz, $PCHCH_3$); $^{13}C\{^1H\}$ NMR (125.7 MHz, C_6D_6, 296 K): $\delta=202.5$ (dt, $^1J_{RhC}=36.\ 7$, $^2J_{PC}=22.4$ Hz, RhC≡), 196.6 (dt, $^1J_{RhC}=41.3$, $^2J_{PC}=14.3$ Hz, $RhC^{q\text{-}IMe}$), 145.57 (s, $C^{q\text{-}Mes}$), 140.21 (s, $C^{q\text{-}Mes}$), 136.0 (s, $C^{q\text{-}Mes}$), 130.08 (s, $C^{q\text{-}Mes}$), 126.07 (s, m-$C^{Mes}H$), 120.55 (s, $C^{IMe}H$), 38.48 (s, $C^{IMe}H_3$), 27.33 (vt, $N=18.2$ Hz, $PCHCH_3$), 23.50 (s, o-$C^{Mes}H_3$), 21.34 (s, p-$C^{Mes}H_3$), 21.20 ppm (s, $PCHCH_3$); $^{11}B\{^1H\}$ NMR (160.4 MHz, C_6D_6, 296 K): $\delta=52$ ppm (s); $^{31}P\{^1H\}$ NMR (202.4 MHz, C_6D_6, 296 K): $\delta=47.1$ ppm (d, $^1J_{RhP}=149.0$ Hz); IR (solid): $\tilde{\nu}=1944$ (C≡C stretch), 1604 cm^{-1} (C=C stretch); UV/Vis (hexane): $\lambda_{max}=205$ nm ($\varepsilon=53\,670$ L mol^{-1} cm^{-1}); elemental analysis calcd (%) for $C_{43}H_{72}BN_2P_2Rh$: C 65.15, H 9.15, N 3.53; found: C 64.83, H 9.26, N 3.51.

X-ray crystallography

Compound 2:

The XRD data of **2** were collected on a Bruker SMART-APEX diffractometer with a CCD area detector and graphite-monochromated $Mo_{K\alpha}$ radiation. The structure was solved by direct methods, refined with the SHELX software package, and expanded by Fourier techniques. All non-hydrogen atoms were refined anisotropically. Hydrogen atoms were included in structure-factor calculations. All hydrogen atoms were assigned to idealized geometric positions. Crystal data for **2**: $C_{42}H_{73}BClOP_2Rh$, $M_r=805.11$; red block, $0.25\times0.23\times0.16$ mm; triclinic, space group $P\bar{1}$; $a=9.8330(16)$, $b=14.350(2)$, $c=16.409(3)$ Å; $\alpha=104.649(2)$, $\beta=96.611(2)$, $\gamma=101.133(2)°$; $V=2164.9(6)$ $Å^3$; $Z=2$; $\rho_{calcd}=1.235$ g cm^{-3}; $\mu=0.559$ mm^{-1}; $F(000)=860$; $T=173(2)$ K, $R_1=0.0487$, $wR_2=0.1151$; 8506 independent reflections ($2\theta\leq52.3°$) and 451 parameters.

Compound 4:

The crystal data of **4** were collected on a Bruker X8-Apex II diffractometer with a CCD area detector and multilayer-mirror-monochromated $Mo_{K\alpha}$ radiation. The structure was solved by direct methods, refined with the SHELX software package, and expanded by Fourier techniques. All non-hydrogen atoms were refined anisotropically. Hydrogen atoms were included in structure-factor calculations. All hydrogen atoms were assigned to idealized geometric positions. The 54 reported least-squares restraints, as shown by the refine ls number restraints key, were attributed to the DELU keyword in ShelXL input ("rigid bond" restraint for all bonds in the connectivity list; standard values of 0.01 for both parameters s1 and s2 were used). The displacement parameters of atoms P2 and P3 of residue 1 and of atoms C1 and C3 of residues 8, 9, 10, 18, 19, and 20 were constrained to the same value. The displacement of atoms P2 and P3 of the residue 1 and of atoms C1 and C3 of the residues 8, 9, 10, 18, 19 and 20 were restrained to the same value with similarity restraint SIMU. The displacement parameters U_{ii} of atoms P2 and P3 of residue 1 and atoms C1 and C3 of residues 8 and 18 were restrained with the ISOR keyword to approximate isotropic behavior. Crystal data for **4**: $C_{43}H_{69}BNP_2Rh$, $M_r=775.65$; red block, $0.384\times0.246\times0.153$ mm; monoclinic space group $P2_1/c$; $a=12.871(9)$, $b=20.354(11)$, $c=16.624(8)$ Å; $\beta=103.10(2)°$; $V=4242(4)$ $Å^3$; $Z=4$; $\rho_{calcd}=1.215$ g cm^{-3}; $\mu=0.507$ mm^{-1}; $F(000)=1656$; $T=100(2)$ K; $R_1=0.0536$, $wR_2=0.0735$; 8338 independent reflections ($2\theta\leq52.04°$) and 530 parameters.

Compound 5:

The crystal data of **5** were collected on a Bruker X8-Apex II diffractometer with a CCD area detector and multilayer-mirror-monochromated $Mo_{K\alpha}$ radiation. The structure was solved by direct methods, refined with the SHELX software package, and expanded by Fourier techniques. All non-hydrogen atoms were refined anisotropically. Hydrogen atoms were included in structure-factor calculations. All hydrogen atoms were assigned to idealized geometric positions. The 348 reported least-squares restraints, as shown by the refine ls number restraints key, were attributed to the DELU keyword in ShelXL input ("rigid bond" restraint for all bonds in the connectivity list; standard values of 0.01 for both parameters s1 and s2 were used). The displacement parameters of atoms P51 to C70 were restrained to the same value with similarity restraint SIMU. The displacement parameters U_{ij} of atoms P51 to C70 were restrained with ISOR keyword to approximate isotropic behavior. Crystal data for **5**: $C_{43}H_{72}BN_2P_2Rh$, $M_r = 792.69$; red block, 0.23 × 0.14 × 0.12 mm; monoclinic, space group $P2_1/c$; $a = 12.8252(4)$, $b = 20.1969(6)$, $c = 16.9479(5)$ Å; $\beta = 101.0450(10)^\circ$; $V = 4308.7(2)$ Å^3; $Z = 4$, $\rho_{calcd} = 1.222$ g cm^{-3}; $\mu = 0.501$ mm^{-1}; $F(000) = 1696$; $T = 100(2)$ K; $R_1 = 0.0369$; $wR_2 = 0.0705$; 8498 independent reflections ($2\theta \leq 52.04^\circ$) and 559 parameters.

CCDC 961895 (**2**), 961896(**4**) and 961897(**5**) contain the supplementary crystallographic data for this paper. These data can be obtained free of charge from The Cambridge Crystallographic Data Centre via www.ccdc.cam.ac.uk/data_request/cif

Acknowledgements

Financial support from the Deutsche Forschungsgemeinschaft is gratefully acknowledged.

Keywords: alkynyl ligands · boron · rhodium · solvatochromism · vinylidene ligands

[1] C. D. Entwistle, T. B. Marder, *Chem. Mater.* **2004**, *16*, 4574 – 4585.
[2] C. D. Entwistle, T. B. Marder, *Angew. Chem.* **2002**, *114*, 3051 – 3056; *Angew. Chem. Int. Ed.* **2002**, *41*, 2927 – 2931.
[3] F. Jäkle, *Coord. Chem. Rev.* **2006**, *250*, 1107 – 1121.
[4] Y. Shirota, M. Kinoshita, T. Noda, K. Okumoto, T. Ohara, *J. Am. Chem. Soc.* **2000**, *122*, 11021 – 11022.
[5] M. Elbing, G. C. Bazan, *Angew. Chem.* **2008**, *120*, 846 – 850; *Angew. Chem. Int. Ed.* **2008**, *47*, 834 – 838.
[6] T. Noda, H. Ogawa, Y. Shirota, *Adv. Mater.* **1999**, *11*, 283 – 285.
[7] M. Haussler, B. Z. Tang, *Adv. Polym. Sci.* **2007**, *209*, 1 – 58.
[8] N. Matsumi, K. Naka, Y. Chujo, *J. Am. Chem. Soc.* **1998**, *120*, 5112 – 5113.
[9] A. Wakamiya, K. Mori, S. Yamaguchi, *Angew. Chem.* **2007**, *119*, 4351 – 4354; *Angew. Chem. Int. Ed.* **2007**, *46*, 4273 – 4276.
[10] Y. Qin, G. L. Cheng, O. Achara, K. Parab, F. Jäkle, *Macromolecules* **2004**, *37*, 7123 – 7131.
[11] V. Cadierno, J. Gimeno, *Chem. Rev.* **2009**, *109*, 3512 – 3560.
[12] R. Wiedemann, P. Steinert, M. Schäfer, H. Werner, *J. Am. Chem. Soc.* **1993**, *115*, 9864 – 9865.
[13] M. Laubender, H. Werner, *Angew. Chem.* **1998**, *110*, 158 – 160; *Angew. Chem. Int. Ed.* **1998**, *37*, 150 – 152.
[14] M. Schäfer, J. Wolf, H. Werner, *Dalton Trans.* **2005**, 1468 – 1481.
[15] H. Werner, *Coord. Chem. Rev.* **2004**, *248*, 1693 – 1702.
[16] M. I. Bruce, *Chem. Rev.* **1991**, *91*, 197 – 257.
[17] M. I. Bruce, *Chem. Rev.* **1998**, *98*, 2797 – 2858.
[18] M. L. Buil, M. A. Esteruelas, K. Garces, E. Oñate, *J. Am. Chem. Soc.* **2011**, *133*, 2250 – 2263.
[19] M. A. Esteruelas, A. M. Lopez, M. Mora, E. Oñate, *Organometallics* **2012**, *31*, 2965 – 2970.
[20] R. Wiedemann, R. Fleischer, D. Stalke, H. Werner, *Organometallics* **1997**, *16*, 866 – 870.
[21] J. Wolf, H. Werner, O. Serhadli, M. L. Ziegler, *Angew. Chem.* **1983**, *95*, 428 – 429; *Angew. Chem. Int. Ed. Engl.* **1983**, *22*, 414 – 416.
[22] C.-W. Chiu, Y. Kim, F. P. Gabbaï, *J. Am. Chem. Soc.* **2009**, *131*, 60 – 61.
[23] Several Rh^I/Rh^{II} redox couples have been reported. See, for example: a) C. Bianchini, F. Laschi, F. Ottaviani, M. Peruzzini, P. Zanello, *Organometallics* **1988**, *7*, 1660 – 1661; b) K. R. Dunbar, S. C. Haefner, *Organometallics* **1992**, *11*, 1431 – 1433; c) D. G. DeWit, *Coord. Chem. Rev.* **1996**, *147*, 209 – 246; d) F. Barrière, W. E. Geiger, *Organometallics* **2001**, *20*, 2133 – 2135.
[24] D. D. Perrin, W. L. F. Armarego, *Purification of Laboratory Chemicals, 3rd ed.*, Pergamon Press, Oxford, **1988**.
[25] T. Schaub, M. Backes, U. Radius, *Organometallics* **2006**, *25*, 4196 – 4206.
[26] C. Busetto, A. Dalfonso, F. Maspero, G. Perego, A. Zazzetta, *J. Chem. Soc. Dalton Trans.* **1977**, 1828 – 1834.

Received: September 19, 2013